doi.org/10.36721/PJPS/2026.40.17091.1

Identification of cultivar-specific markers for Zhangtouhong citri reticulatae pericarpium by integrated GC-MS, electronic nose and HPLC profiling

Liujin Wu[1,2], Jiamin Liang[1], Peiyang Hu[1], Lili Huang[3], Min Zhang[4] and Meng Gao[1,2]*

[1]Jiangxi University of Traditional Chinese Medicine, Nanchang 330002, Jiangxi, China
[2]National Pharmaceutical Engineering Center for Solid Preparation in Chinese Herbal Medicine, Nanchang 330006, Jiangxi, China
[3]Jiangxi Academy of Forestry, Nanchang 330032, Jiangxi, China
[4]Nanchang Inspection and Testing Center, Nanchang Key Laboratory of Quality Control and Safety Evaluation of TCM, Nanchang 330015, Jiangxi, China

Abstract: **Background**: Most quality control frameworks and aging studies on *Citri Reticulatae Pericarpium* (CRP) are based on mainstream cultivars, particularly Chachi mandarin. Zhangtouhong, a local citrus from Jiangxi Province, has received little systematic attention regarding its cultivar-specific traits and aging-related chemical changes; applying Chachi-derived criteria may thus bias its quality assessment. **Objectives**: Aging-related changes in key constituents were compared between Zhangtouhong and Chachi CRP to identify shared aging features, cultivar-specific traits and candidate cultivar-specific markers for Zhangtouhong quality evaluation. **Methods**: Samples of both cultivars aged for 3, 5 and 10 years were analyzed. Five core volatile oil components were quantified by volatile oil determination with GC-MS; holistic odor fingerprints were captured by electronic nose; shared volatile profiles were characterized by HS-GC-MS; and six representative flavonoids were quantified by HPLC. Cultivar, aging year and interaction effects were evaluated using two-factor linear models, Spearman correlation, PCA, PLS-DA, OPLS-DA and PERMANOVA. Candidate cultivar-specific markers were screened through an integrated multi-criteria approach. **Results**: Volatile oil yields remained relatively stable across aging, with D-limonene dominating in both cultivars, whereas myrcene and γ-terpinene showed divergent aging patterns. Electronic nose fingerprints clearly separated the two cultivars, with eight sensors contributing most. HS-GC-MS identified 40 shared volatiles, with alkenes forming the common aromatic backbone. Integrated screening yielded 16 cultivar-specific volatile markers, among which methyl 2-(methylamino) benzoate, linalool and α-thujene were prioritized. Among flavonoids, hesperidin was strongly associated with aging duration, while nobiletin, 5-demethylnobiletin and sinensetin showed high discriminative power for cultivar differentiation. **Conclusion**: Zhangtouhong and Chachi CRP exhibit both common aging-related chemical changes and marked cultivar-dependent differences. CRP quality markers should therefore be distinguished as candidate common aging markers and cultivar-specific markers. Systems built solely on Chachi cannot fully capture Zhangtouhong characteristics, underscoring the need for cultivar-adapted quality evaluation methods.

Keywords: *Citri reticulatae pericarpium*; Cachi cultivar; Cultivar specificity; Candidate cultivar-specific markers; Zhangtouhong cultivar

Submitted 02-07-2026 – Revised 06-09-2026 – Accepted 02-10-2026

Article in Press

INTRODUCTION

Dried and aged citrus peel, *Citri Reticulatae Pericarpium*, or CRP, has been a staple in traditional Chinese medicine and functional foods for centuries (Xu *et al.*, 2026). The old saying that "CRP gets better with age" underscores just how central aging duration is to its quality. As the peels age, volatiles, flavonoids and other secondary metabolites keep transforming. These shifts build the characteristic aroma, taste and overall sensory profile and they likely influence bioactivity and the dual medicinal–edible value. In the past few years, research on CRP quality has surged. However, most current knowledge comes from Guangchenpi, specifically from the Chachi cultivar. Teasing apart how key constituents change over time, while keeping cultivar background in mind, is therefore essential for understanding quality formation and for building reliable evaluation methods.

Researchers have turned to chromatography, mass spectrometry and sensor-based tools to track how aging affects CRP quality. GC-MS and GC-IMS are the workhorses for volatile changes, while liquid chromatography–mass spectrometry handles non-volatiles, flavonoids in particular. Meanwhile, electronic noses, backed by chemometrics, can distinguish CRP samples by aging period, origin, or cultivar based on smell alone, offering a technical hand in identifying aging stages and assessing quality (Luo *et al.*, 2017; Alim *et al.*, 2026; Zhang *et al.*, 2026). Among the chemical players, volatiles and flavonoids represent two major material bases: the former largely shape aroma and its evolution, while the

**Corresponding author:* e-mail: whajim@sina.com

latter tie closely to active constituent accumulation, pharmacological relevance and taste quality (Hu *et al.*, 2025).

When it comes to quality evaluation and aging research on *Citri Reticulatae Pericarpium* (CRP), the spotlight has long been on Guangchenpi, specifically the Chachi cultivar from Xinhui, Guangdong (Zhang *et al.*, 2025). Now, consider Zhangtouhong, a local cultivar from Zhangshu, Jiangxi. It's already part of the local specialty industry and its peels have been used as medicinal CRP for ages. It has been reported that its chemical makeup differs from that of other citrus varieties. Given that Zhangtouhong differs from Chachi in germplasm, cultivation background and how it's traditionally used, copying the Chachi evaluation framework over to it may not capture its cultivar-specific quality traits and could easily lead us astray. At present, a systematic picture of how Zhangtouhong's chemistry shifts during aging is still lacking. No side-by-side comparison with Chachi on quality markers has been reported to date. The present study was therefore designed to compare the chemical profiles of these two cultivars across multiple aging time points. The aim, at least at this stage, was to identify the cultivar-specific components that set Zhangtouhong apart from Chachi and to provide experimental grounding for quality evaluation methods suited to locally distinctive CRP resources.

To address this, Zhangtouhong and Chachi CRP samples aged for 3, 5 and 10 years were selected for side-by-side comparison. GC-MS analysis of essential oil components, HS-GC-MS profiling of shared volatiles, electronic nose odor fingerprinting, flavonoid quantification by HPLC and chemometric analysis were combined to compare how volatile characteristics, flavonoid profiles and overall odor responses evolve with aging in the two cultivars. The aim was to clarify the cultivar-specific aging features of Zhangtouhong, separate candidate common markers from cultivar-specific ones and to identify key differential constituents that carry both statistical weight and discriminative power. These insights should provide a scientific footing for establishing quality markers for Zhangtouhong and for standardizing the evaluation of locally distinctive CRP resources. At the same time, they offer a reference for moving beyond the Guangchenpi-dominated paradigm toward quality methods that better accommodate cultivar diversity.

MATERIALS AND METHODS

Zhangtouhong and Chachi Chenpi samples with different aging years were systematically characterized using E-nose, HS-GC-MS, GC-MS and HPLC analyses, followed by multivariate statistical analysis and data integration. This integrated approach was designed to characterize aging-related compositional changes, distinguish inter-cultivar differences and identify potential cultivar-specific markers.

Sources of CRP samples

All CRP samples were authenticated as *Citri Reticulatae Pericarpium* (CRP) by Professor Lili Huang from the Jiangxi Academy of Forestry. A total of 16 CRP samples were included in this study and classified into two groups according to cultivar. The Zhangtouhong cultivar group (sample codes C1–C8) was collected from Xin'gan County, Jiangxi Province, whereas the Chachi cultivar group (sample codes C9–C16) was obtained from Xinhui County, Guangdong Province. Three aging gradients, namely 3, 5 and 10 years, were included for both groups. Specifically, each group contained four samples aged for 3 years and two samples each aged for 5 and 10 years. Detailed information on all samples is provided in table 1.

Experimental materials

The D-limonene reference standard was purchased from Macklin Biochemical Co., Ltd. (Shanghai, China).

Reference standards of (−)-β-pinene and terpinolene were obtained from TCI Chemical Industry Development Co., Ltd. (Shanghai, China). γ-Terpinene and p-cymene (4-isopropyltoluene) reference standards were obtained from Aladdin Biochemical Technology Co., Ltd. (Shanghai, China). The myrcene reference standard was purchased from Yuanye Biotechnology Co., Ltd. (Shanghai, China). Acetonitrile (HPLC grade) and n-hexane (HPLC grade) were obtained from Tedia Company Inc. (Fairfield, OH, USA). Anhydrous sodium sulfate (AR grade) was obtained from Xilong Scientific Co., Ltd. An AR5120 microbalance and an MS205DU analytical balance were both manufactured by Mettler-Toledo (Greifensee, Switzerland). A SuperNose electronic nose system was supplied by Ruibin International Trade Co., Ltd. (Shanghai, China). A 7000C triple quadrupole gas chromatography–mass spectrometer (GC-MS/MS) was obtained from Agilent Technologies Inc. (Santa Clara, CA, USA). A GC×GC/qMS-TQ8040 comprehensive two-dimensional gas chromatography–tandem mass spectrometer equipped with an AOC-6000Plus autosampler was purchased from Shimadzu Corp. (Kyoto, Japan).

Volatile oil extraction and quantification of representative volatile components

Volatile oil was extracted according to General Regulation 2204, Method A, for volatile oil determination in the Pharmacopoeia of the People's Republic of China (2025 Edition). Briefly, 50 g of each powdered sample, passed through a No. 2 sieve, was placed in a round-bottom flask, mixed with eight volumes of distilled water and heated under reflux for 5 h. The volatile oil yield was calculated after extraction using the following equation 1:

$$\text{Yield}\ (\%) = \frac{\text{Volume of volatile oil (mL)}}{\text{Weight of sample (g)}} * 100\% \quad (1)$$

Article in Press

Table 1: Detailed source information of citri Reticulatae Pericarpium samples.

Sample code	Aging year	Cultivar	Geographical origin	Sample code	Aging year	Cultivar	Geographical origin
C1	3 years	Zhangtouhong	Xin'gan, Jiangxi Province	C9	3 years	Chachi	Xin'hui, Guangdong Province
C2	3 years	Zhangtouhong	Xin'gan, Jiangxi Province	C10	3 years	Chachi	Xin'hui, Guangdong Province
C3	3 years	Zhangtouhong	Xin'gan, Jiangxi Province	C11	3 years	Chachi	Xin'hui, Guangdong Province
C4	3 years	Zhangtouhong	Xin'gan, Jiangxi Province	C12	3 years	Chachi	Xin'hui, Guangdong Province
C5	5 years	Zhangtouhong	Xin'gan, Jiangxi Province	C13	5 years	Chachi	Xin'hui, Guangdong Province
C6	5 years	Zhangtouhong	Xin'gan, Jiangxi Province	C14	5 years	Chachi	Xin'hui, Guangdong Province
C7	10 years	Zhangtouhong	Xin'gan, Jiangxi Province	C15	10 years	Chachi	Xin'hui, Guangdong Province
C8	10 years	Zhangtouhong	Xin'gan, Jiangxi Province	C16	10 years	Chachi	Xin'hui, Guangdong Province

D-limonene and myrcene were quantified using the external standard method. Reference standards of D-limonene (120.33 mg), myrcene (40.41 mg), γ-terpinene (80.04 mg), (−)-β-pinene (40.39 mg), terpinolene (40.32 mg) and p-cymene (4-isopropyltoluene, 40.12 mg) were accurately weighed and transferred into separate 10 mL volumetric flasks. Each standard was dissolved and diluted to volume with n-hexane to prepare stock solutions at final concentrations of 12033, 4041, 8004, 4039, 4032 and 4012 μg/mL, respectively. All stock solutions were stored at 4 °C in a refrigerator (Haier, model BCD-630WGHSS95SMU1, China) until use. Working calibration solutions were prepared by accurately pipetting appropriate volumes of each stock solution into 10 mL volumetric flasks and diluting to volume with n-hexane.

An accurately weighed 50 mg aliquot of each volatile oil sample was transferred into a 5 mL volumetric flask and diluted to volume with n-hexane. Anhydrous sodium sulfate was added to remove residual moisture and the mixture was vortexed until homogeneous. The solution was filtered through a 0.45 μm microporous membrane filter to obtain a volatile oil sample solution at a concentration of 10 mg/mL. The filtrate was then transferred into an autosampler vial for GC-MS analysis.

Chromatographic separation was performed using high-purity helium as the carrier gas. The injection volume was 1 μL and the split ratio was set at 20:1. The oven temperature program was as follows: the initial temperature was maintained at 40 °C for 5 min, increased to 100 °C at 1.5 °C/min, then increased to 250 °C at 80 °C/min and held for 2 min. Mass spectrometric detection was performed in electron impact (EI) ionization mode at an electron energy of 70 eV. The ion source temperature was set at 230 °C, the quadrupole temperature at 150 °C and the mass scan range at m/z 20–550(Xu *et al.*, 2026; Xie *et al.*, 2025; Jo *et al.*, 2023).

Electronic nose analysis

An accurately weighed 0.5 g aliquot of sample powder, prepared as described in Section 2.1, was transferred into a 40 mL headspace vial and equilibrated at room temperature for 12 h to enrich volatile components in the vial headspace. Before sample detection, the electronic nose system was preheated for 1 h. The instrumental parameters were set as follows: sensor cleaning time, 180 s; inlet gas flow rate, 0.6 L/min; detection duration, 120 s; and sample injection volume, 10 mL. Each sample was analyzed in triplicate. Response signals from 14 sensors (S1–S14) were collected. Among them, sensor S1 was mainly sensitive to aromatic compounds; S2 primarily responded to nitrogen oxides and low-molecular-weight amines; S4 was associated with organic acid esters and terpenes; S6 was related to sterols and triterpenes; and S11 was responsive to volatile organic compounds (Cui *et al.*, 2026; Wang *et al.*, 2023). Detailed specifications of each sensor are summarized in supplementary table S1.

HS-GC-MS analysis

For headspace GC-MS analysis, 1.0 g of sample powder was transferred into a 25 mL headspace vial using a GCMS-QP2020 NX gas chromatograph-mass spectrometer (Shimadzu, Kyoto, Japan). The headspace conditions were as follows: the vial was heated at 120 °C with an equilibration time of 10 min; the loop temperature was 130 °C; the transfer line temperature was 140 °C; the pressure equilibration time was 0.5 min; and the injection duration was 0.5 min. Separation was performed on an SH-i-5SIL MS capillary column (30 m × 0.25 mm, 0.25 μm film thickness) with the injector at 230 °C in splitless mode and helium carrier gas at a constant flow rate of 1.00 mL/min. The oven program started at 40 °C for 5 min, rose to 200 °C at 3 °C/min and was held for 5 min.

Article in Press

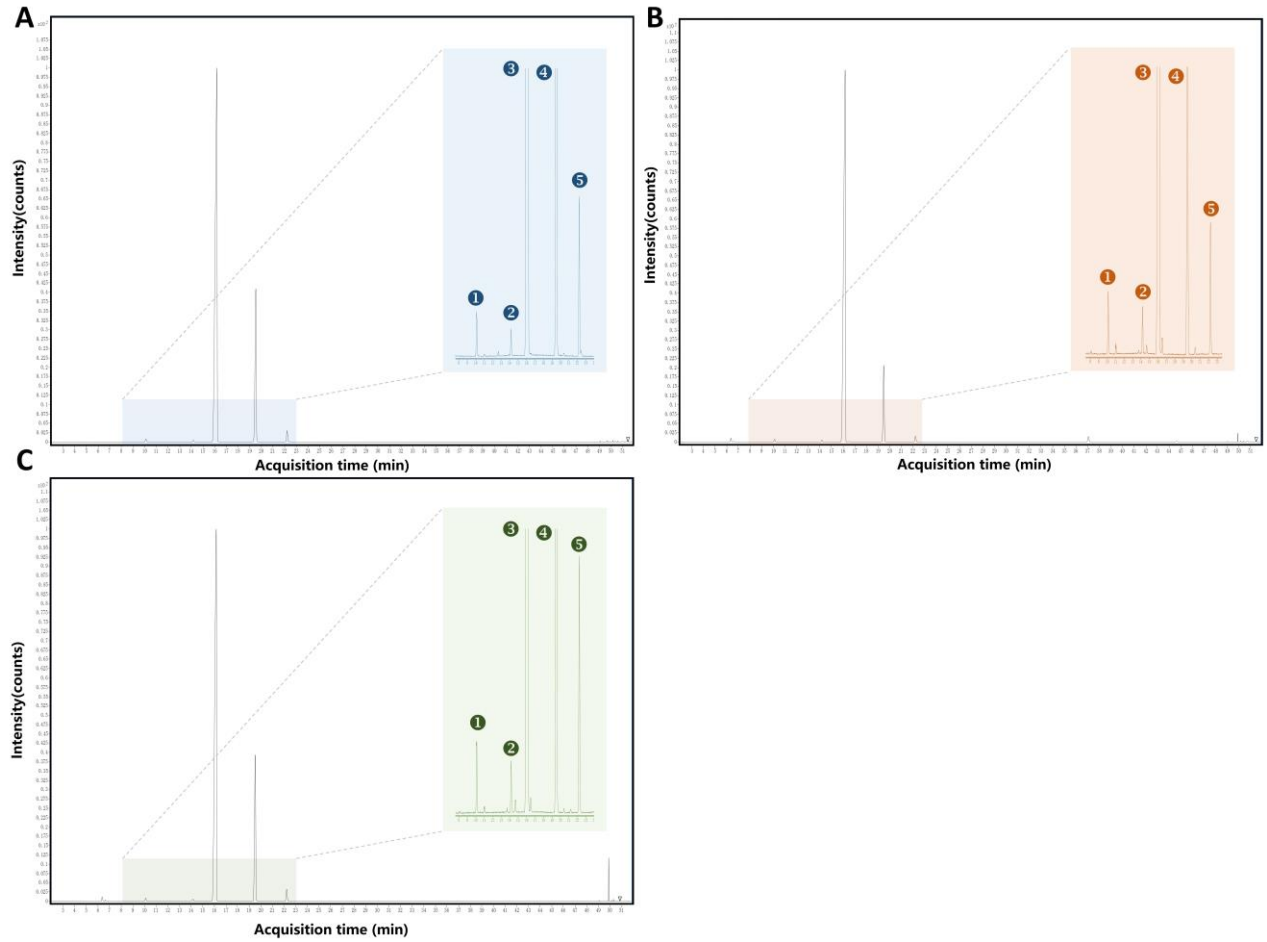


Fig. 1: GC-MS total ion chromatograms (TIC) of volatile oil samples. (A) TIC of mixed reference standards; (B) TIC of Zhangtouhong cultivar sample; (C) TIC of Chachi cultivar sample. Peaks: 1, (−)-β-pinene; 2, Terpinolene; 3, D-limonene; 4, γ-Terpinene; 5, Myrcene. These five monoterpenes represent the core volatile oil components quantified in this study. Retention times and peak patterns were consistent between the reference standards and both sample groups, confirming the identity of the core components.

Mass detection used EI ionization (70 eV), with the ion source at 200 °C, the interface at 220 °C and full-scan mode over *m/z* 35–400(Li *et al.*, 2025; Deng *et al.*, 2022).

Quantification of representative flavonoids

Accurately weighed standards of hesperidin, narirutin, nobiletin, tangeretin, sinensetin and 5-demethylnobiletin were dissolved in methanol to prepare individual stock solutions (approximately 1.0 mg/mL). Equal volumes of each stock solution were mixed to obtain the mixed reference standard solution. For extraction, 0.5 g of sample powder was placed in a stoppered conical flask, 50 mL of methanol was added and the flask was weighed and reflux-extracted at 70 °C for 1 h. After cooling to room temperature, the lost mass was replenished with methanol and the solution was homogenized and filtered through a 0.22 μm membrane before injection. Chromatographic separation was performed on a PFchrom EP C18 column (250 mm × 4.6 mm, 5 μm particle size, 120 Å pore size). The mobile phases were acetonitrile (A) and 0.1% (v/v) phosphoric acid aqueous solution (B). The gradient elution program was as follows: 0–8 min, 20% A; 8–23 min, linear gradient from 20% to 45% A; 23–40 min, 45% A; and 40–45 min, linear gradient from 45% to 60% A. Detection wavelengths were set at 283 nm and 330 nm, the flow rate was 1.0 mL/min, the column temperature was controlled at 30 °C and the injection volume was 5 μL (Martinidou *et al.*, 2024; Li *et al.*, 2022).

Data processing and statistical analysis

All statistical analyses and data visualizations in this study were performed using R software, Origin 2026 and SIMCA 14.1. Volatile oil yield was summarized using descriptive statistics. For the quantitative data of the five core volatile oil components and the response datasets of the 14 electronic nose sensors, a two-factor linear model was constructed using cultivar and aging year as independent variables. Multiple testing correction was performed using the Benjamini–Hochberg procedure and adjusted statistical significance was expressed as the false discovery rate

Article

(FDR). Spearman rank correlation analysis was further conducted within each cultivar group to investigate the variation trends of each indicator with aging duration. For the global data matrices obtained from electronic nose and HS-GC-MS analyses, permutational multivariate analysis of variance (PERMANOVA) was applied to evaluate the effects of cultivar, aging year and their interaction on the overall flavor-related chemical profiles. Using the contents of six flavonoid components as core variables, line graphs, box plots and clustered heatmaps were generated in Origin 2026 for visual comparison. Principal component analysis (PCA) and orthogonal partial least squares discriminant analysis (OPLS-DA) were performed using SIMCA 14.1. Differential flavonoid markers associated with the aging process of CRP were screened using the criteria of variable importance in projection (VIP) value > 1 and $P < 0.05$.

RESULTS

Comparative analysis of volatile characteristics

Changes in essential oil yield and core essential oil components

The GC-MS total ion chromatograms (TICs) showed consistent retention times and peak patterns between the reference standards and the two sample groups. The five core essential oil components were identified as (−)-β-pinene, terpinolene, D-limonene, γ-terpinene and myrcene (Fig. 1). The volatile oil yields of the two sample groups ranged from 3.8% to 4.4%. The average yields of the 3-, 5- and 10-year aged samples were 4.25%, 4.00% and 4.20% in the Zhangtouhong group and 3.95%, 3.90% and 4.10% in the Chachi group, respectively, with only minor fluctuations across aging periods (Fig. 2A; Table S2). Quantitative analysis of the five core essential oil components showed that D-limonene was the predominant component in both groups (Cai *et al.*, 2026; Shi *et al.*, 2024). In the Zhangtouhong group, D-limonene content decreased from 231.15 ± 24.53 mg/g to 178.97 ± 1.29 mg/g and terpinolene content decreased from 5.57 ± 0.67 mg/g to 4.53 ± 0.08 mg/g. In the Chachi group, D-limonene content decreased from 256.16 ± 58.74 mg/g to 203.94 ± 4.00 mg/g, while terpinolene content decreased from 6.83 ± 1.96 mg/g to 4.70 ± 0.13 mg/g. By contrast, the variation trends of γ-terpinene and myrcene were not fully consistent between the two groups and (−)-β-pinene also showed evident fluctuations (Figs. 2B and 2C; Table S3).

Two-way linear model analysis showed that myrcene and γ-terpinene exhibited significant cultivar effects, aging year effects and cultivar × year interaction effects. (−)-β-Pinene mainly showed a significant interaction effect. Although D-limonene and terpinolene showed decreasing mean concentrations, their overall main cultivar effects were not statistically significant (Table S4). Spearman rank correlation analysis within each group further showed that, in the Zhangtouhong group, (−)-β-pinene was significantly positively correlated with aging year, whereas terpinolene and D-limonene were significantly negatively correlated with aging year. In the Chachi group, D-limonene and terpinolene also showed decreasing trends, but the correlations were not statistically significant after multiple-testing correction. Principal component analysis (PCA) showed that the first two principal components cumulatively explained 98.6% of the total variance. The PCA score plot displayed partial separation between the two groups, although considerable overlap remained (Fig. 2D). The Z-score heatmap showed that the five core components were shared by both groups, with D-limonene consistently showing the highest relative abundance, followed by terpinolene and the other three components. The 3-year aged Chachi samples showed relatively higher levels of γ-terpinene, myrcene and (−)-β-pinene, corresponding to their distribution away from the other samples in the PCA space (Fig. 2E). Overall, the five core essential oil components mainly reflected shared variation patterns and localized differences between the two cultivar groups, with limited separation between cultivars.

Differences in overall odor fingerprints based on electronic nose analysis

The heatmap of electronic nose responses showed that, except for sensor S14, the Zhangtouhong group generally exhibited higher response intensities than the Chachi group on most sensors. More pronounced differences were observed for sensors S1, S2, S5, S6, S7, S9, S10 and S11 (Fig. 3A). Faceted box plots further showed that sensors S11, S6, S2 and S9 maintained relatively stable inter-group differences across aging periods, with higher signal intensities in the Zhangtouhong group and lower overall responses in the Chachi group (Fig. 3B). According to the sensor annotations, these response differences were associated with odor dimensions related to aromatic compounds, nitrogen oxides and low-molecular-weight amines, sterols and triterpenes, volatile organic compounds and selected oxygenated aliphatic hydrocarbon derivatives (Luo *et al.*, 2017, Wang *et al.*, 2023). In the volcano plot, all statistically significant sensors except S14 showed negative $\log_2$ fold change values, corresponding to higher electronic nose response intensities in the Zhangtouhong group under the present experimental conditions (Fig. 3C). PCA of the electronic nose data showed that the first two principal components cumulatively explained 91.0% of the total variance and the two groups formed a relatively clear separation along the first principal component (Fig. 3D). Partial least squares discriminant analysis (PLS-DA) showed a similar distribution pattern, with samples from the two groups located on opposite sides of Component 1 and showing limited overlap (Fig. 3E). Furthermore, the 200 permutation tests showed that the R^2Y and Q^2 of the random permutation model were lower than those of the original model and both $p(R^2Y)$ and $p(Q^2)$ were < 0.01, indicating that the PLS-DA model was statistically significant and the risk of overfitting was low.

Article in Press

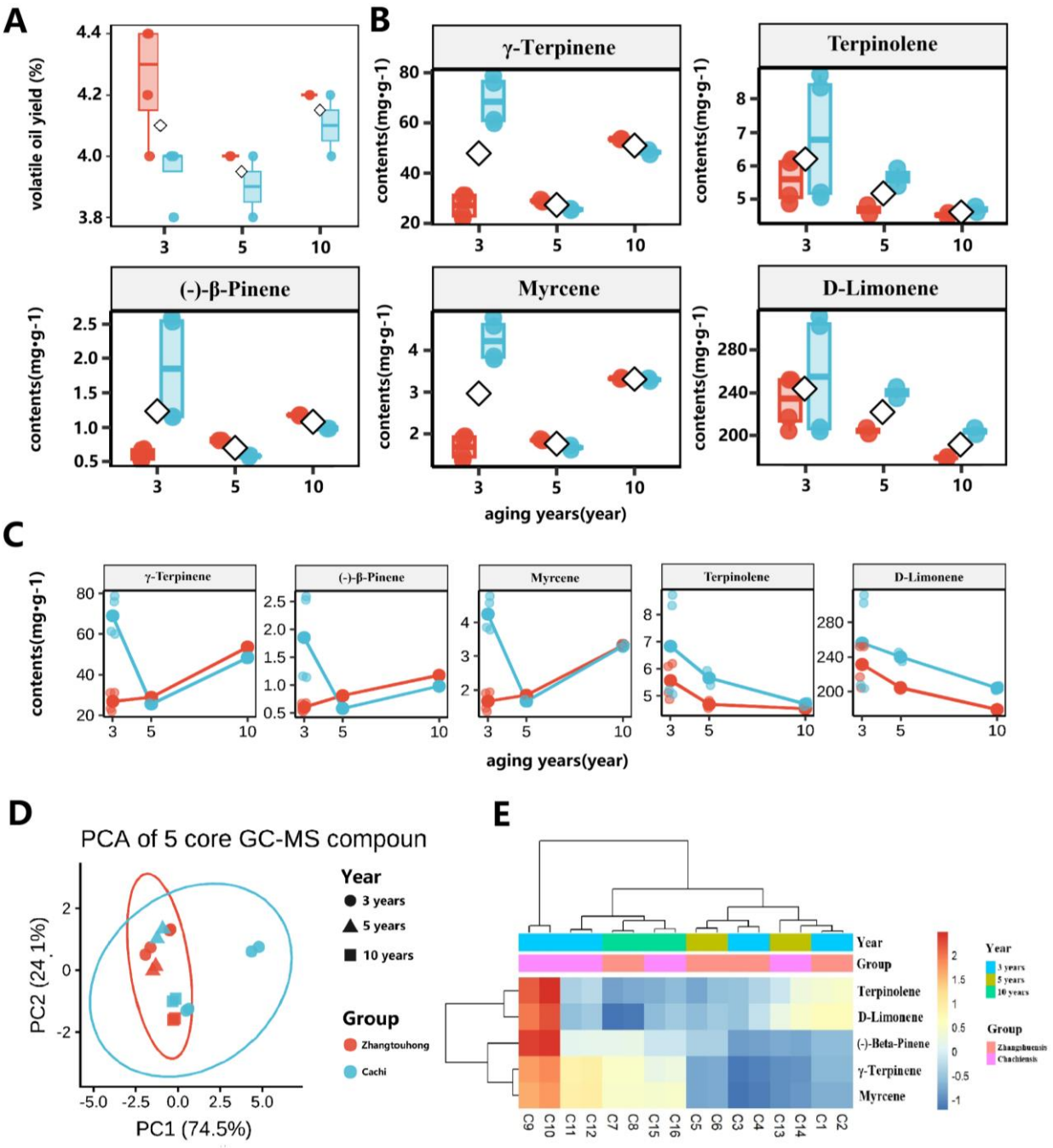


Fig. 2: Comprehensive analysis of volatile oil components in Zhangtouhong and Chachi CRP samples across three aging periods (3, 5 and 10 years). (A) Box plot of volatile oil yield for each cultivar (Red: Zhangtouhong; Clue: Chachi); (B) Box plots of the contents of the five core volatile oil components (D-limonene, γ-terpinene, myrcene, terpinolene and (−)-β-pinene). Color coding follows the same scheme as in (A). All subfigures share the same x-axis titles and unit; (C) Variation trend profiles of volatile oil component contents during aging. Solid lines connect the mean values at each aging year (Red: Zhangtouhong; Blue: Chachi). All subfigures share the same x- and y-axis titles and units; (D) Principal component analysis (PCA) score plot based on the five core volatile components. Ellipses indicate the 95% confidence regions for each cultivar (Red circles: Zhangtouhong; Blue triangles: Chachi). The percentages in the axis labels indicate the proportion of variance explained by PC1 and PC2; (E) Heatmap of the contents of the five core volatile components. Rows represent components and columns represent individual samples grouped by cultivar and aging year. The color scale ranges from blue (low relative content) to red (high relative content), with Z-score normalization applied to each row.

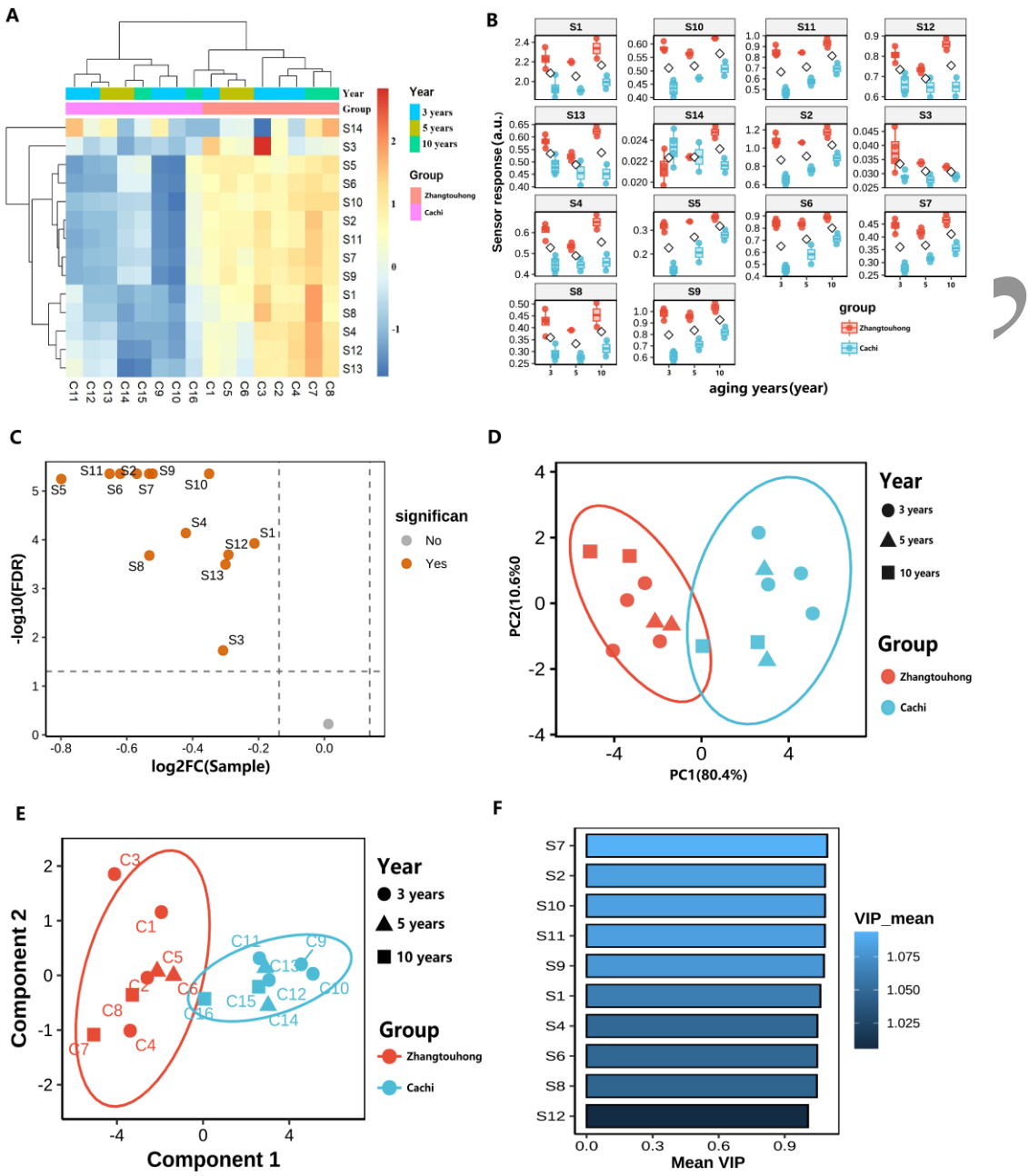


Fig. 3: Comprehensive analysis of electronic nose odor fingerprints of Zhangtouhong and Chachi CRP samples. (A) Heatmap of responses from 14 electronic nose sensors. Rows represent sensors (S1–S14), columns represent individual samples grouped by cultivar and aging year. Color scale indicates normalized response intensity (Z-score), ranging from blue (low) to red (high); (B) Comparison of response values across the 14 sensors. Blue, Zhangtouhong; red, Chachi. All subfigures share the same x- and y-axis titles and units; (C) Volcano plot of inter-group differential sensors. Each point represents one sensor. The x-axis shows $\log_2$ fold change and the y-axis shows-$\log_{10}$ (FDR-adjusted P-value). Dashed horizontal line indicates the significance threshold (FDR < 0.05); dashed vertical lines indicate $|\log_2$ fold change$| > 0.5$. Sensors meeting both criteria are colored red; non-significant sensors are gray; (D) PCA score plot based on the 14 sensor responses. Ellipses indicate 95% confidence regions for each cultivar. Red, Zhangtouhong; blue, Chachi. Percentages in axis labels denote variance explained by PC1 and PC2; (E) PLS-DA score plot. The x-axis represents Component 1, which captures inter-group separation between cultivars; the y-axis represents Component 2, which captures within-group variation. Points are colored and shaped as in (D); (F) Variable importance in projection (VIP) ranking of sensors from the PLS-DA model. Bars represent VIP values and the dashed horizontal line indicates the conventional threshold of VIP > 1. Sensors with VIP > 1 are considered to have significant discriminative contribution.

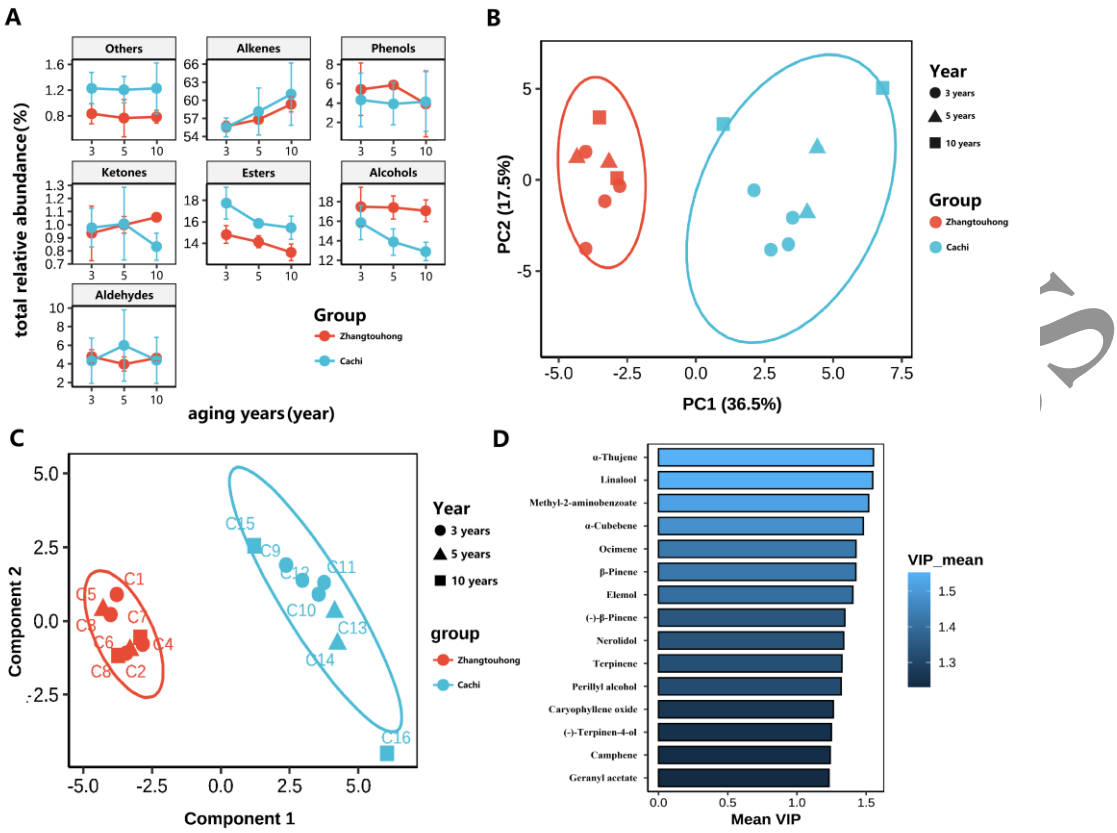


Fig. 4: Comprehensive analysis of HS-GC-MS volatile profiling in Zhangtouhong and Chachi CRP samples. (A) Relative abundance of chemical classes (alkenes, alcohols, esters, aldehydes, ketones, phenols and others) among the 40 shared volatile components across the three aging years (3, 5 and 10 years). Bars represent the mean relative abundance of each chemical class; error bars indicate standard deviation. Red bars, Zhangtouhong; blue bars, Chachi. All subfigures share the same x- and y-axis titles and units; (B) Principal component analysis (PCA) score plot based on centered log-ratio (CLR)-transformed relative abundances of the 40 shared volatile components. Each point represents one sample. Red, Zhangtouhong; blue, Chachi. Ellipses indicate 95% confidence regions for each cultivar. Percentages in the axis labels denote the proportion of variance explained by PC1 and PC2; (C) Partial least squares discriminant analysis (PLS-DA) score plot. Component 1 primarily separates the two cultivars, while Component 2 captures within-group variation. Points are colored and shaped as in (B): red, Zhangtouhong; blue, Chachi; (D) Variable importance in projection (VIP) ranking of the 40 shared volatile components from the PLS-DA model. Bars represent VIP values and the dashed horizontal line indicates the conventional threshold of VIP > 1. Components with VIP > 1 are considered to have significant discriminative contribution to cultivar separation.

Permutational multivariate analysis of variance (PERMANOVA) showed that the cultivar factor accounted for 67.86% of the total variance ($P < 0.05$), whereas neither the aging year effect nor the cultivar × year interaction effect reached statistical significance ($P > 0.05$). Ranking of variable importance in projection (VIP) scores showed that sensors S7, S2, S10, S11, S9 and S1 had the highest VIP values, with S7 ranking first. When VIP scores were considered together with univariate statistical significance, sensors S7, S2, S10, S11, S9, S1, S4, S6, S8 and S12 were retained as response variables with both statistical significance and discriminative contribution (Fig. 3F). Univariate linear model analysis based on sensor response values showed that 13 of the 14 sensors, all except S14, exhibited significant main cultivar effects, with the strongest effects observed for S11, S6, S2, S9, S10, S7 and S5. In addition, sensors S11, S6, S2, S9, S10, S7 and S5 also showed significant main effects of aging year (Table S5).

Volatile compound profile characteristics based on HS-GC-MS analysis

Approximately 768 chromatographic peaks were detected by HS-GC-MS analysis. After spectral matching against the NIST mass spectral library, filtering by relative abundance threshold and screening for components commonly detected in both groups, 169 volatile components were preliminarily identified and 40 shared volatile components were selected for subsequent integrative analysis. These 40 shared components were mainly classified as alkenes, alcohols, aldehydes and esters, with smaller proportions of ketones, phenols and other compounds (Luo *et al.*, 2017; Song *et al.*, 2024) (Table S6).

Article

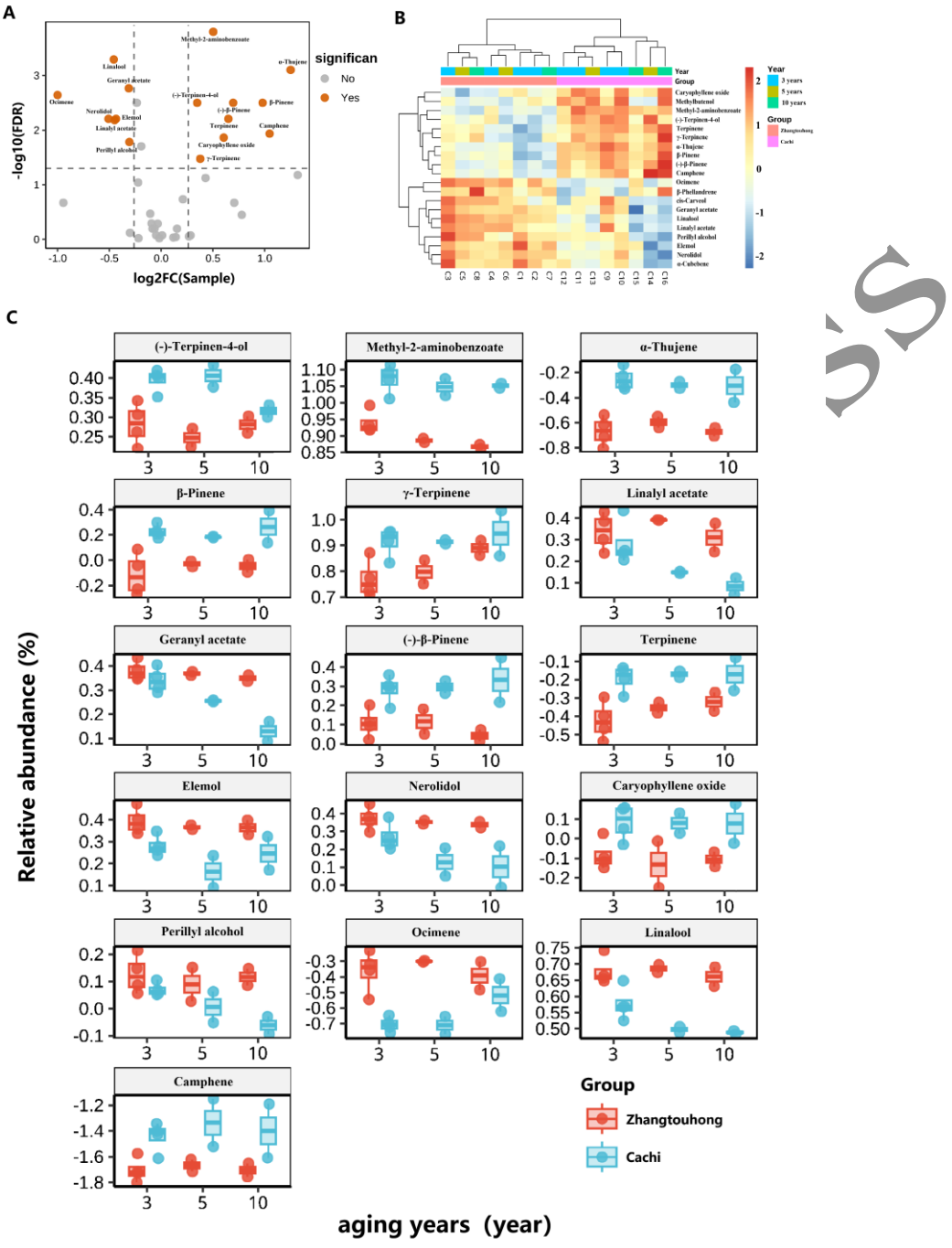


Fig. 5: Screening analysis of differential volatile markers from HS-GC-MS profiling. (A) Volcano plot of differential volatile components between Zhangtouhong and Chachi. Each point represents one volatile component. The x-axis shows $\log_2$ fold change and the y-axis shows $-\log_{10}$ (FDR-adjusted P-value). Dashed horizontal line indicates the significance threshold (FDR < 0.05), dashed vertical lines indicate $|\log_2 \text{fold change}| > 0.5$. Red points represent components significantly enriched in Zhangtouhong, blue points represent components significantly enriched in Chachi and gray points are not statistically significant; (B) Heatmap of the 16 candidate differential volatile markers. Rows represent individual markers and columns represent samples grouped by cultivar and aging year (3, 5 and 10 years). Color scale indicates Z-score-normalized relative abundance, ranging from blue (low) to red (high). Red, Zhangtouhong; blue, Chachi; (C) Box plots of selected differential markers (methyl 2-(methylamino) benzoate, linalool, α-thujene, β-pinene, (−)-β-pinene, caryophyllene oxide, geranyl acetate, ocimene, elemol, nerolidol, linalyl acetate, perillyl alcohol, (−)-4-terpineol, terpinene, camphene and γ-terpinene). Red boxes, Zhangtouhong; blue boxes, Chachi. Only markers with consistently large inter-cultivar differences are shown for clarity. All subfigures share the same x- and y-axis titles and units

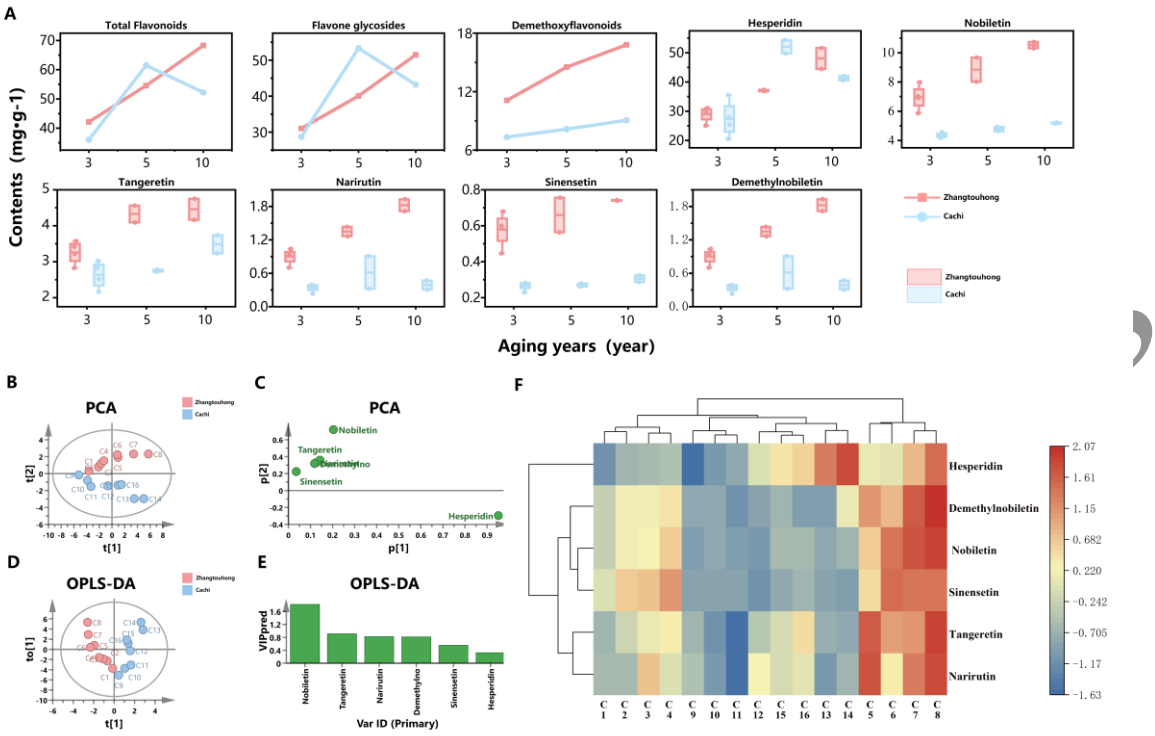


Fig. 6: Comprehensive analysis of flavonoid components in Zhangtouhong and Chachi CRP samples across three aging periods (3, 5 and 10 years). (A) Line chart and box plots of flavonoid contents. Line chart showing the mean contents of flavonoid glycosides and demethoxyflavonoids across aging years. Solid red lines, Zhangtouhong; solid blue lines, Chachi. Box plots showing individual flavonoid contents. Red, Zhangtouhong; blue, Chachi. All subfigures share the same x- and y-axis titles and units; (B) PCA score plot based on the contents of six flavonoid components. Each point represents one sample. Red, Zhangtouhong; blue, Chachi. Ellipses indicate 95% confidence regions for each cultivar. Percentages in the axis labels denote the proportion of variance explained by PC1 and PC2; (C) PCA loading plot. Each vector represents one flavonoid component; the direction and length of the vector indicate its contribution to the principal components; (D) Orthogonal partial least squares discriminant analysis (OPLS-DA) score plot. The x-axis represents the predictive component that separates the two cultivars; the y-axis represents the orthogonal component that captures within-group variation. Points are colored and shaped as in (B): red, Zhangtouhong; blue, Chachi; (E) Variable importance in projection (VIP) ranking from the OPLS-DA model. Bars represent VIP values for each flavonoid component and the dashed horizontal line indicates the conventional threshold of VIP > 1. Components with VIP > 1 are considered to have significant discriminative contribution to cultivar separation; (F) Heatmap of the contents of six flavonoid components. Rows represent individual flavonoids (hesperidin, narirutin, nobiletin, tangeretin, sinensetin and 5-demethylnobiletin) and columns represent samples grouped by cultivar and aging year. The color scale indicates Z-score-normalized content, ranging from blue (low) to red (high). The top annotation bar marks the cultivar identity of each sample (Red: Zhangtouhong; Blue: Chachi).

In the relative abundance profiles of the 40 shared volatile components, alkenes showed the highest relative abundance across all aging stages. The average relative abundances of alkenes in 3-, 5- and 10-year aged Zhangtouhong samples were 55.70%, 56.86% and 59.36%, respectively, while the corresponding values in Chachi samples were 55.53%, 58.15% and 61.05%. For alcohols, the Zhangtouhong group remained at approximately 17% throughout aging, whereas the Chachi group decreased from 15.84% to 12.90%. For esters, the relative abundance decreased from 14.82% to 13.16% in the Zhangtouhong group and from 17.75% to 15.45% in the Chachi group (Fig. 4A; Table S6). After centered log-ratio (CLR) transformation of the 40 shared components, PCA showed that the first two principal components cumulatively explained 54.0% of the total variance. The two groups showed separation along the first principal component axis (Fig. 4B). PLS-DA also showed differentiation between the Zhangtouhong and Chachi groups along Component 1 (Fig. 4C). Permutation test showed that R^2Y and Q^2 of the randomized model were lower than those of the original model and $p(R^2Y)$ and $p(Q^2)$ were both < 0.01, indicating that the PLS-DA model was statistically significant. PERMANOVA indicated a significant cultivar effect, explaining 21.72% of the total variance, whereas neither the aging year effect nor the cultivar × year interaction reached statistical significance (Table S7). VIP ranking showed that α-thujene, linalool, methyl 2-(methylamino) benzoate, α-cubebene, ocimene, β-pinene, elemol, (−)-β-pinene, nerolidol and terpinene had high discriminative contributions to inter-cultivar separation (Fig. 4D; Table S7).

Article in Press

Combined screening of volatile candidate cultivar-specific markers

To identify more robust cultivar-specific markers, a combined screening strategy integrating mean variable importance in projection (VIP) scores, FDR-adjusted inter-group differences and fold change values was applied. A total of 16 cultivar-specific markers were obtained (Table S8). Representative compounds with higher relative abundance in the Chachi group included methyl 2-(methylamino) benzoate, α-thujene, β-pinene, (−)-β-pinene, (−)-4-terpineol, terpinene, camphene, caryophyllene oxide and γ-terpinene. By contrast, linalool, geranyl acetate, ocimene, elemol, nerolidol, linalyl acetate and perillyl alcohol showed higher relative abundance in the Zhangtouhong group. Among these compounds, methyl 2-(methylamino)benzoate, linalool and α-thujene showed both significant univariate differences and high VIP rankings.

The volcano plot showed that cultivar-specific markers were distributed on both sides of the $\log_2$ fold change axis. α-thujene and β-pinene showed higher relative abundance in the Chachi group, whereas linalool, geranyl acetate, ocimene and elemol showed higher relative abundance in the Zhangtouhong group (Fig. 5A). The hierarchical clustering heatmap showed that the 16 cultivar-specific markers largely separated samples according to cultivar grouping (Fig. 5B). Box plots showed distinct aging-related variation patterns among individual markers. Methyl 2-(methylamino) benzoate remained at consistently high levels in the Chachi group throughout aging; linalool showed higher overall abundance in the Zhangtouhong group; and (−)-β-pinene, β-pinene and caryophyllene oxide consistently showed higher levels in the Chachi group across all aging stages (Fig. 5C).

Comparative analysis of flavonoid components

Changes in the content profiles of flavonoid components

Quantitative analysis of the six flavonoid components showed distinct flavonoid variation patterns between the Zhangtouhong and Chachi groups during aging (Table S8; Fig. 6A). In the Zhangtouhong group, the contents of both flavonoid glycosides and demethoxyflavonoids increased synchronously with aging duration. The total content and relative proportion of demethoxyflavonoids were consistently higher in the Zhangtouhong group than in the Chachi group. In the Chachi group, flavonoid glycosides showed a phased pattern, with an increase at the 5-year aging stage followed by a decrease at the 10-year stage. Demethoxyflavonoids in the Chachi group showed a gradual increase throughout aging (Fig. 6A). Single-component analysis showed that hesperidin was the main contributor to variation in total flavonoid glycosides, whereas 5-demethylnobiletin was the dominant component contributing to changes in total demethoxyflavonoids. Overall correlation analysis showed that aging duration was significantly positively correlated with the contents of hesperidin, narirutin and tangeretin. Among these indicators, hesperidin showed the highest sensitivity to aging duration ($P = 0.005$) (Table S9).

Screening of flavonoid candidate cultivar-specific markers

PCA was performed using the flavonoid composition data of the two cultivar groups across different aging durations. The PCA score plot showed that the Zhangtouhong group was generally distributed along the positive axis of PC1, whereas the Chachi group was mainly located along the negative axis of PC1, showing separation between the two cultivars. With prolonged aging, PC1 scores of the Zhangtouhong group increased progressively. In contrast, 5-year aged Chachi samples showed higher scores along PC2, corresponding to the phased increase in hesperidin content (Fig. 6B). According to the PCA loading results, nobiletin and 5-demethylnobiletin contributed strongly to the separation between Zhangtouhong and Chachi, whereas hesperidin showed a greater association with aging-related variation (Fig. 6C). To further screen key variables for distinguishing the two groups, orthogonal partial least squares discriminant analysis (OPLS-DA) was conducted. The OPLS-DA score plot showed separation between the Zhangtouhong and Chachi groups (Fig. 6D). In the permutation test, R^2Y and Q^2 of the randomized model were lower than those of the original model and $p(Q^2)$ was less than 0.01, indicating that the discrimination effect of the model was not caused by the randomized group and the risk of overfitting was relatively low. VIP analysis showed that nobiletin, with a VIP value greater than 1, was the highest-ranked variable for differentiating the two cultivars. Its content was higher in the Zhangtouhong group and was also associated with aging year and the cultivar × year interaction effect. By contrast, hesperidin had the lowest VIP value and showed no significant overall difference between the two cultivars, corresponding to its stronger association with aging duration rather than cultivar grouping (Fig. 6E). To visualize flavonoid content differences between Zhangtouhong and Chachi at different aging stages, bidirectional hierarchical clustering analysis was performed after Z-score normalization. The samples were broadly divided into two clusters corresponding to the Zhangtouhong and Chachi groups. In the Zhangtouhong group, the overall levels of sinensetin, nobiletin, tangeretin, 5-demethylnobiletin and narirutin were relatively high and increased with extended aging. In the Chachi group, these components were generally present at lower levels, while the 5-year aged Chachi samples were mainly characterized by elevated hesperidin content. Indicator clustering showed that sinensetin and nobiletin had the closest clustering relationship and 5-demethylnobiletin was also closely associated with this module. Hesperidin was distantly clustered from the other indicators and exhibited a relatively independent variation pattern (Fig. 6F).

Article in Press

Table 2: Predictive analysis of cultivar-specific markers in CRP.

Candidate markers	Role in this study	Reported in other citrus varieties	Implication	Reference
D-Limonene	Stable; dominant in both cultivars	Dominant volatile in most Citrus reticulata peels	Common aging feature	(Fan *et al*., 2024) (Yu *et al*., 2022)
Myrcene	Divergent aging trajectory between cultivars	Reported in various Citrus peels; levels vary with origin and cultivar	Shared compound with cultivar-specific aging behavior	(Yang *et al.*, 2022) (Du Lingling *et al.*, 2025) (Zhang *et al*., 2026)
γ-Terpinene				
Methyl 2-(methylamino) benzoate	Distinct aging trends between cultivars	Chachi-specific compounds	Strong cultivar-specific candidate	(Liu *et al*., 2025b)
Linalool		Widely reported in citrus volatiles; cultivar-dependent abundance	Shared compound, but cultivar-distinct trajectory	(Galvan-Lima *et al*., 2021)
α-Thujene	Distinct profile in Zhangtouhong	Limited reports in CRP	Potentially Zhangtouhong-specific	(Wang *et al*., 2023) (Phuong and Le Pham Tan Quoc, 2025)
Hesperidin	Tracks aging duration in both cultivars	Widely reported in citrus	Shared compound	(Martinidou *et al*., 2024)
Nobiletin	Strong differential signal between cultivars	Highly variable among cultivars	Cultivar-sensitive marker	(Brits *et al.*, 2021) (Fang *et al.*, 2022) (Peng *et al.*, 2021) (Li *et al.*, 2025)
5-Demethylnobiletin		Reported in aged CRP; cultivar-dependent accumulation		
Sinensetin		Reported in certain mandarin cultivars; not universally dominant		(Lin *et al*., 2026)

DISCUSSION

In this study, Zhangtouhong and Chachi CRP were compared across multiple analytical dimensions: volatile oil yield, core volatiles, e-nose fingerprints, HS-GC-MS profiles and flavonoids. The results showed a dual picture: shared aging trends alongside pronounced cultivar-dependent differences. It seems that CRP from different citrus types does not follow a single aging script. Volatile oil yields stayed relatively flat across 3 to 10 years, with no steady rise or fall. D-limonene dominated the profile in both cultivars, confirming that monoterpenes form the common chemical backbone (Luo *et al*., 2017; Cai *et al*., 2026). This is not merely a statistical observation: D-limonene is a major aromatic contributor in citrus peels and has well-documented antioxidant, anti-inflammatory and gastroprotective properties (Li *et al.*, 2024; Yang *et al.*, 2023; Senthil Kumar *et al*., 2025). However, its sheer abundance made it a poor cultivar discriminator, it works better as a shared quality indicator. In contrast, myrcene and γ-terpinene displayed partially divergent trajectories, hinting at cultivar-specific aging dynamics. These acyclic monoterpenes are more chemically reactive than D-limonene and contribute fresh, herbaceous and mildly spicy notes to citrus aroma; their differential decline likely reflects cultivar-dependent oxidation or isomerization pathways during storage. So, the core oil components gave us a glimpse of common terpenoid ground and some local differences, but a handful of high-abundance compounds could not fully capture Zhangtouhong's unique aging features.

What the electronic nose told us, however, was much clearer. Zhangtouhong CRP consistently generated stronger sensor responses and the holistic odor fingerprints separated the cultivars cleanly. This makes sense: an e-nose captures the integrated response from many volatiles, offering a more global aroma picture than a few targeted compounds (Poornima *et al*., 2025; Baietto and Wilson, 2015). Indeed, PERMANOVA, VIP and univariate analyses all pointed to cultivar as the dominant factor, with sensors S7, S2, S10, S11, S9, S1, S6 and S5 leading the charge. Aging year modulated the intensity within each cultivar but did not shuffle the overall pattern. From these data, it is pretty clear that Zhangtouhong has its own odor identity, one that a Chachi-only evaluation system would miss (Chen *et al.*, 2024).

Article in Press

The volatile profiling by HS-GC-MS backed up the e-nose findings at the molecular level. Among the 40 shared volatiles, monoterpene hydrocarbons (alkenes) formed the common aroma backbone, consistent with the terpenoid-rich nature of citrus (Liu *et al.*, 2025). But, Chachi showed a more marked drop in alcohols and esters with aging, compounds linked to floral and fruity notes. Their decline could mirror a shift from fresh, fruity aromas toward the more aged, medicinal, or woody character typical of CRP (Zhang *et al*., 2025). That points to distinct changes in aroma during aging. Multivariate analysis again highlighted cultivar as the major source of variance. It can therefore be concluded that Zhangtouhong and Chachi differed in the characteristics of their volatile components during aging, rather than merely in total volatile abundance.

On this basis, the 16 cultivar-specific markers obtained by integrated screening further defined the characteristic volatile signatures of the two CRP cultivars. The Chachi group was characterized by relatively higher levels of methyl 2-(methylamino)benzoate and several monoterpene-related compounds, including α-thujene, β-pinene, (−)-β-pinene and terpinene. Methyl 2-(methylamino)benzoate is an aromatic ester with a distinctive grape-like odor and has been reported as a key contributor to the characteristic aroma of certain citrus peels, its elevated presence in Chachi may partly explain the cultivar's recognized sensory profile. In contrast, the Zhangtouhong group was distinguished by elevated levels of oxygenated terpenoids and ester components, such as linalool, geranyl acetate, ocimene, elemol, nerolidol and linalyl acetate. Linalool and its ester derivatives are widely recognized for their floral, sweet aroma and have documented calming, anti-inflammatory and antimicrobial effects (Huan *et al.*, 2024; Fan *et al.*, 2024; An *et al.*, 2021). Elemol and nerolidol are sesquiterpene alcohols with more persistent woody-floral notes and also exhibit antifungal and antioxidant properties (Glumac *et al.*, 2023; Arunachalam *et al.*, 2021). Thus, the cultivar-specific volatile profiles are not merely statistical artifacts; they reflect genuine differences in biosynthetic emphasis, Chachi leaning toward hydrocarbon monoterpenes and a distinctive aromatic ester, Zhangtouhong toward oxygenated and esterified terpenoids, which may translate into divergent sensory and functional properties. Among these markers, methyl 2-(methylamino)benzoate (Yu *et al.*, 2022; Li *et al.*, 2023; GAN *et al.*, 2025), linalool (DU *et al.*, 2025; GAN *et al*., 2025) and α-thujene (Song *et al*., 2024) showed both significant univariate differences and high discriminative contributions, making them high-priority candidate markers within the current sample cohort. Overall, the volatile differences between the two CRP cultivars were mainly reflected in cultivar-specific volatile compound profiles. This finding suggests that the conventional volatile marker system derived from Chachi CRP may not adequately represent the aging characteristics of Zhangtouhong CRP and supports the need to consider cultivar-specific volatile indicators in CRP quality evaluation.

Flavonoid profiles further revealed differences between the two cultivars, with cultivar again identified as the major factor contributing to these differences. Univariate statistics, PCA, OPLS-DA and clustering all pointed to cultivar-dependent aging (Peng *et al.*, 2025; Luo *et al.*, 2023). In Zhangtouhong, both flavonoid glycosides (Im *et al.*, 2024) and demethoxyflavonoids (Toledo *et al.*, 2024) rose together as aging progressed. Moreover, the total amount and relative proportion of demethoxyflavonoids were higher in Zhangtouhong than in Chachi. This is phytochemically noteworthy because demethoxyflavonoids, particularly 5-demethylnobiletin, have been reported to exhibit stronger anticancer activity than the corresponding fully methoxylated flavonoids (Yanping *et al.*, 2022; Chen *et al.*, 2022). Their preferential accumulation in Zhangtouhong therefore suggests not only a compositional difference but also a potentially distinct bioactivity profile. In Chachi, flavonoid glycosides showed a phased pattern, up at 5 years, down at 10, while demethoxyflavonoids increased gradually. This asynchrony suggests that Chachi aging involves a different interplay between flavonoid subclasses. Hesperidin proved to be a robust aging-responsive marker, whereas nobiletin, 5-demethylnobiletin and sinensetin consistently discriminated the cultivars. Collectively, Zhangtouhong did not simply recapitulate the Chachi flavonoid aging pattern; instead, it exhibited a characteristic accumulation of demethoxyflavonoids and a coordinated rise across multiple subclasses. For quality assessment, this indicates that hesperidin content alone is insufficient and that cultivar-specific flavonoid panels should be considered.

To better assess the potential relevance of the markers identified here, representative volatile and flavonoid compounds were compared with previous reports in other citrus cultivars (Table 2). This comparison highlights which compounds represent common citrus constituents and which show stronger cultivar-dependent behavior, thereby providing additional support for the selection of candidate cultivar-specific markers for Zhangtouhong.

A few limitations are worth acknowledging here. The sample size was on the small side, 16 samples in total, spanning two cultivars and three aging periods. So the cultivar-specific markers that emerged from the various statistical and chemometric analyses should probably be treated as preliminary candidates rather than definitive markers ready for broad application. Future work ought to cast a wider net: more geographical origins, more production batches, more aging periods and independent validation cohorts to test whether these candidates actually hold up across batches and conditions. Another point worth noting is the aging window itself. This study examined samples aged only 3–10 years, so longer-term materials

Article in Press

will be needed to build a fuller picture of how the chemistry changes as different CRP cultivars age.

CONCLUSION

Taken together, these findings indicate that different chemical indicators serve different purposes in CRP quality evaluation. (Yu *et al.*, 2024). D-limonene, the monoterpene hydrocarbon backbone and hesperidin mainly reflect shared aging features. Meanwhile, the 16 differential volatile markers, key e-nose sensor responses and flavonoids such as nobiletin, 5-demethylnobiletin and sinensetin reflect the differential aging features between Zhangtouhong and Chachi CRP. The implication is straightforward: quality standards developed from Chachi CRP should not be blindly applied to every CRP cultivar. Marker systems should be built to accommodate both shared aging trends and cultivar-distinct chemical profiles. For Zhangtouhong, paying more attention to its characteristic volatile odor profile and flavonoid remodeling pattern will pave the way toward a quality evaluation strategy that truly fits this local cultivar. After all, a Zhangtouhong peel should not be judged solely by Chachi-derived criteria; the present data support a more cultivar-adaptive evaluation approach.

Future studies should systematically validate these candidate markers using larger sample populations collected from multiple production regions and different batches, together with independent validation cohorts. On this basis, their application value in the quality control of Zhangtouhong CRP could be further explored. For example, these candidate markers may be incorporated into fingerprinting profiles or quantitative detection systems to distinguish CRP samples derived from different cultivars and to provide chemical evidence for identifying geographical origin confusion, cultivar substitution, or adulteration. With the accumulation of multi-regional and multi-batch validation data, these markers may also provide scientific support for the development of regulatory standards, standardized cultivation, optimization of aging processes and quality control of decoction pieces of Zhangtouhong CRP, thereby facilitating the establishment of a more cultivar-adaptive quality evaluation framework for Zhangtouhong CRP.

Acknowledgments
During the preparation of this manuscript, the authors used ChatGPT for initial language polishing of the first draft. The manuscript was subsequently rewritten and substantively edited by a scholar with overseas research experience to ensure accuracy and fluency. The authors take full responsibility for the integrity, originality and accuracy of the content and no AI tool was listed as an author or used for any generative purpose beyond language assistance.

Authors' contributions
Liujin Wu: Writing - original draft, methodology, investigation and conceptualization; Jiamin Liang: Visualization, software and data curation; Peiyang Hu: Methodology and data curation; Lili Huang: Resources and investigation; Min Zhang: Writing - review and editing and validation; Meng Gao: Writing - review and editing, project administration and investigation. All authors have read and approved the published version of this manuscript.

Funding
This research was supported by the Jiangxi Provincial Key Research and Development Program (No. 20252BCG330010 and No. 20252BCG330012), the Jiangxi Provincial Research Center for Traditional Chinese Medicine Standards (No. 12425013) and the Jiangxi University of Chinese Medicine Science and Technology Innovation Team Development Program (No. CXTD22001).

Data availability statement
All data generated or analysed during this study are included in this published article.

Ethical approval
Not applicable. This study did not involve human participants, animal experiments, or clinical samples. All experiments were conducted using chemical reagents and standard analytical methods.

Conflict of interest
The authors declare no conflict of interest.

REFERENCES

Alim A, Huang C, Zhao X, Gaowa S, Zhang R, Zhang J, Zhang X, Jin Y and Hu W (2026). Investigating the impact of different drying methods on the aroma of citri Reticulatae Pericarpium using GC-MS/GC-IMS and E-nose technology. *Foods.,* **15**(7): 1117.

An Q, Ren J, Li X, Fan G, Qu S, Song Y, Li Y and Pan S (2021), Recent updates on bioactive properties of linalool. *Food Funct.,* **12**(21): 10370-10389.

Arunachalam S, Nagoor Meeran MF, Azimullah S, Sharma C, Goyal SN and Ojha S (2021). Nerolidol attenuates oxidative stress, inflammation and apoptosis by modulating Nrf2/MAPK signaling pathways in doxorubicin-induced acute cardiotoxicity in rats. *Antioxidants (Basel),* **10**(6): 984.

Baietto M and Wilson AD (2015). Electronic-nose applications for fruit identification, ripeness and quality grading. *Sensors (Basel).*, **15**(1): 899-931.

Brits M, Naessens T, Theunis M, Taktak O, Allouche N, Pieters L and Foubert K (2021). Identification and quantification of polymethoxylated flavonoids in different citrus species using UPLC-QTOF-MS/MS and

Article in Press

HPLC-DAD. *Planta Med.*, **15**(1): 899-931.

Cai A, Diao N, Zhang X, Zhang J, Zhang R, Huang C, Alim A, Jin Y, Zhao X, Feng K, Hu W and Sarengaowa (2026). Biological dynamics and application prospects of Citri Reticulatae Pericarpium (CRP): A medicine and food perspective review. *Front Pharmacol.*, **17**: 1793560.

Chen P, Fu R, Shi Y, Liu C, Yang C, Su Y, Lu T, Zhou P, He W, Guo Q and Fei C (2024), Optimizing BP neural network algorithm for Pericarpium Citri Reticulatae (Chenpi) origin traceability based on computer vision and ultra-fast gas-phase electronic nose data fusion. *Food Chem.*, **442**: 138408.

Chen Q, Gu Y, Tan C, Sundararajan B, Li Z, Wang D and Zhou Z (2022). Comparative effects of five polymethoxyflavones purified from *Citrus tangerina* on inflammation and cancer. *Front Nutr.*, **9**:963662.

Cui C, Sun L, Huang X, Nie Z, Zhu Y, Wang L, Yang Y, Xing X and Ke F (2026). Integrated metabolomic and transcriptomic analyses reveal aroma diversity and its regulatory networks in aromatic acidic citrus. *Front Plant Sci.*, **17**: 1785725.

Deng H, He R, Huang R, Pang C, Ma Y, Xia H, Liang D, Liao L, Xiong B, Wang X, Zhang M, Ao X, Yu B, Han D and Wang Z (2022). Optimization of a static headspace GC-MS method and its application in metabolic fingerprinting of the leaf volatiles of 42 citrus cultivars. *Front Plant Sci.*, **13**: 1050289.

Du L, Meng X, Hu Y, Liu R, Zhang S, Zhong L, Zhu W and Liang Y (2025). Integration of electronic nose and headspace gas chromatography-mass spectrometry for differentiating the volatile compositions of Citri Reticulatae Pericarpium made from *Citrus reticulata* Blanco var. zhany shuensis f.Aged for Different Years. *Food Sci., China Food Publ. Co.*, **46**(11): 253-262.

Fan Z, Jeffries KA., Sun X, Olmedo G, Zhao W, Mattia MR, Stover E, Manthey JA, Baldwin EA, Lee S, Gmitter FG, Plotto A and Bai J (2024). Chemical and genetic basis of orange flavor. *Sci Adv.*, **10**(9): eadk2051.

Fang H, Zhang H, Wei X, Ye X and Tian J (2022). Phytochemicals and antioxidant capacities of young citrus fruits cultivated in China. *Molecules.*, **27**(16): 5185.

Galvan-Lima N, Cunha SC, Martins ZE, Soares AG, Ferreira IMPL and Farah A (2021). Headspace volatolome of peel flours from citrus fruits grown in Brazil. *Food Res Int.*, **150**(Pt B): 110801.

Gan J, Ai J, Xu X, Xue Q, Zou J, Zhang Q, He S, Yang Y, Fu W, Jin H and Liang X (2025). Quality analysis of citri reticulatae pericarpium based on UPLC-Q-TOF-MS/MS and quantitative fingerprinting. *Mod. Chin. Med.*, **27**(7): 1262-1272.

Glumac M, Ike Uli V, Marinovi Terzi I and Radan M (2023). Mechanism of cis-nerolidol-induced bladder carcinoma cell death. *Cancers (Basel).*, **15**(3): 981.

Hu Y, Hu D, Yin L, Deng Z, Cheng Y, Li H, Wang F and Liu Y (2025). Dynamic profiling of bioactive compounds, flavor metabolites and quality-related microorganisms during the freshening-drying-aging process of citri reticulatae pericarpium: Implications for quality formation mechanisms. *Food Chem X.*, **30**: 102906.

Huan C, Feifei L, Yanru Z, Zhiyue Y, Jin C, Shiguo C and Xingqian Y (2024). The flavor characterization of 'Huyou' (*Citrus changshanensis*) essential oils extracted by conventional and novel methods. *Agriculture (Basel, Switz.)*, **14**(1): 131.

Im ST, Kang H, Kim J, Kim S, Kim K and Lee S (2024). Narirutin-Rich celluclast extract from mandarin (*Citrus unshiu*) peel alleviates high-fat diet-induced obesity and promotes energy metabolism in C57BL/6 mice. *Int J Mol Sci.*, **25**(8): 4475.

Jo SM, Hong SJ, Yoon S, Jeong H, Youn MY and Shin E (2023). Comparative study on volatile compounds and taste components of various citrus cultivars using electronic sensors, GC-MS and GC-olfactometry. *Food Sci Biotechnol.*, **33**(8): 1825-1837.

Li D, Yu X, Wei Q, Yin Z, Yu Y, Li Y and Yan J (2025). Effects of botanical-geographical origin and storage time on the composition of free and bound polymethoxyflavones in dried citrus peels. *Food Chem.*, **496**(Pt 1): 146599.

Li P, Yao X, Zhou Q, Meng X, Zhou T and Gu Q (2022). Citrus peel flavonoid extracts: Health-beneficial bioactivities and regulation of intestinal microecology *in-vitro*. *Front Nutr.*, **9**: 888745.

Li T, Chen K, Wang X, Wang Y, Su Y and Guo Y (2023). Mass spectrometry rearrangement ions and metabolic pathway-based discovery of indole derivatives during the aging process in Citrus reticulata 'Chachi'. *Foods.*, **13**(1): 8.

Li X, Gao Q, Liu Z, Yao L, Ren X and Kong Q (2025). Identification and profiling of volatiles using headspace-solid-phase microextraction/gas chromatography-mass spectrometry and headspace gas chromatography-ion mobility spectrometry to reveal early contamination progress of sour rot in citrus. *J Agric Food Chem.*, **73**(21): 12591-12603.

Li Y, Li W, Ye Z, Ji C and Zhou Z (2024). Antioxidant, anti-inflammatory and anticancer activities of five citrus peel essential oils. *Antioxidants (Basel).*, **13**(12): 1562.

Lin D, Zhang J, Chen M, Zhong C, Cao H, Ma Z, Wu M and Zhang Y (2026). Identification of Citri reticulatae pericarpium (chenpi) from different cultivars via lc-ms/ms and UPLC coupled with multivariate chemometrics analysis. *Food Sci Nutr.*, **14**(3): e71591.

Liu Y, Wen H, Hu Z, Liu X, Chen Q, Wen T, Liang Y, Hu Y, Zeng J, Chen J and Xu J (2025). CreSAMT1 is mainly responsible for the biosynthesis of characteristic aroma compound dimethyl anthranilate in Citrus reticulata 'Chachiensis'. *Hortic Res.*, **13**(3): uhaf331.

Luo J, Liang L, Xie Q, Qiu Y, Jiang S, Yang Y, Zhu L, Fu Y, Chen S, Wang W and Yuan H (2023). Differential analysis of phytochemistry and antioxidant activity in

Article in Press

five citrus by-products based on chromatography, mass spectrometry and spectrum-effect relationships. *Food Chem X*, **20**: 101010.

Luo M, Luo H, Hu P, Yang Y, Wu B and Zheng G (2017). Evaluation of chemical components in Citri Reticulatae Pericarpium of different cultivars collected from different regions by GC-MS and HPLC. *Food Sci Nutr.*, **6**(2): 400-416.

Martinidou E, Michailidis M, Ziogas V, Masuero D, Angeli A, Moysiadis T, Martens S, Ganopoulos I, Molassiotis A and Sarrou E (2024). Comparative evaluation of secondary metabolite chemodiversity of citrus genebank collection in Greece: Can the peel be more than waste?. *J Agric Food Chem*, **72**(16): 9019-9032.

Peng M, Deng J, Xu J, Chen B, Deng X, Cai Y, Liu W and Zheng G (2025). Influence of storage environments and packaging materials on the bioactive compounds in Citri Reticulatae Pericarpium. *Food Sci Nutr.*, **13**(6): e70393.

Peng Z, Zhang H, Li W, Yuan Z, Xie Z, Zhang H, Cheng Y, Chen J and Xu J (2021). Comparative profiling and natural variation of polymethoxylated flavones in various citrus germplasms. *Food Chem.*, **354**: 129499.

Phuong LBB and Quoc LPT (2025). Assessment of biological activity and physicochemical composition of essential oils from selected Citrus species in Vietnam. *Food Sci. Preserv.*, **32**(6): 1091-1100.

Poornima S, Habiba U, Shafi Z, Noor A, Pandey VK and Singh R (2025). Understanding the Concepts of Smart E-Nose technology in combination with machine learning for new era of food safety: An advanced Review. *Food Saf. Health.*, **3** (4): 518–534.

Senthil Kumar KJ, Gokila Vani M, Dakpa G and Wang S (2025). Dietary limonene promotes gastrointestinal barrier function via upregulating tight/adherens junction proteins through cannabinoid receptor type-1 antagonistic mechanism and alters cellular metabolism in intestinal epithelial cells. *Biofactors.*, **51**(1): e2106.

Shi J, Peng L, Chen W, Qiao W, Wang K, Xu Y and Cheng J (2024). Evaluation of chemical components and quality in Xinhui Chenpi (Citrus reticulata 'Chachi') with two different storage times by GC-MS and UPLC. *Food Sci Nutr.*, **12**(7): 5036-5051.

Song Z, Xu J, Tian J, Deng J, Deng X, Peng M, Luo W, Wei M, Li Y and Zheng G (2024). Differentiating tangerine peels from other *Citrus reticulata* through GC-MS, UPLC-Q-Exactive Orbitrap-MS and HPLC-PDA. *ACS Omega.*, **10**(1): 1688-1704.

Toledo R, Tomas-Navarro M, Yuste JE, Crupi P and Vallejo F (2024). An update on citrus polymethoxyflavones: Chemistry, metabolic fate and relevant bioactivities. *Eur. Food Res. Technol.*, **250**: 2179-2192.

Wang M, Li X, Ding H, Chen H, Liu Y, Wang F and Chen L (2023). Comparison of the volatile organic compounds in *Citrus reticulata* 'Chachi' peel with different drying methods using E-nose, GC-IMS and HS-SPME-GC-MS. *Front Plant Sci*, **14**: 1169321.

Wang P, Wang H, Zou J, Chen L, Chen H, Hu Y, Wang F and Liu Y (2023). Electronic Nose and Head Space GC-IMS provide insights into the dynamic changes and regularity of volatile compounds in Zangju (*Citrus reticulata* cv. Manau Gan) Peel at Different Maturation Stages. *Molecules.*, **28**(14): 5326.

Xie Y, Zhang L, Wu W, Xie J, Gao B, Xiao Y and Zhu D (2025). Sustainable and green extraction of citrus peel essential oil using intermittent solvent-free microwave technology. *Bioresour Bioprocess.*, 12(1):48.

Xu X, He H, Jia S, Sun Y, Sun T and Lang Y (2026). Recent advances in Citri Reticulatae Pericarpium polysaccharides: Extraction, structure, bioactivity and applications: A review. *Int J Biol Macromo.*, **337**(Pt 1): 149543.

Yang F, He L, Shen M, Wang F, Chen H and Liu Y (2022). A Correlation between Pericarpium Citri Reticulatae volatile components and the change of the coexisting microbial population structure caused by environmental factors during aging. *Front Microbiol.*, **13**: 930845.

Yang J, Lee S, Jang S, Kim K and Park M (2023). Anti-inflammatory effects of essential oils from the peels of citrus cultivars. *Pharmaceutics.*, **15**(6):1595.

Yanping X, Ting Z, Man Z, Ruiqiang Z, Siyue Z, Dongli L, Denggao Z, Yanyan M, ChiTang H and Qingrong H (2022). 5-Demethylnobiletin and its major metabolites: Efficient preparation and mechanism of their anti-proliferation activity in HepG2 cells. *Food Sci. Hum. Wellness.*, **11**(5): 1191-1200.

Yu P, Zeng Y, Li C, Qiu B, Shi Y, He Q, Lesmes U and Achmon Y (2024). Quality Change of Citri Reticulatae Pericarpium (Pericarps of Citrus reticulata 'Chachi') during storage and its sex-based *in-vitro* digestive performance. *Foods.*, **13**(22): 3671.

Yu X, Chen X, Li Y and Li L (2022). Effect of drying methods on volatile compounds of *Citrus reticulata* Ponkan and Chachi peels as characterized by GC-MS and GC-IMS. *Foods.*, **11**(17): 2662.

Zhang J, Zhang Y, Li B, Chen C, Jia S and Liu Y (2026). Mechanism of quality formation in aged citri reticulatae pericarpium: A multi-omics study integrating HS-SPME-GC-MS, HS-GC-IMS, E-nose and microbiome analysis. *Lwt-food Sci. Technol.*, **247**: 119340.

Zhang W, Zhang H, Chen X, Liu T, Fu X, Nie Q and Li X (2025). Metabolomic insights into the aging process of Citrus reticulata cv. ' Dahongpao ' peel. *Int. J. Food Prop.*, **28**(1): 2576156.

Article in Press